

Influence of thermostats and carrier gas on simulations of nucleation

Jan Wedekind

*Institut für Physikalische Chemie, Universität zu Köln, Luxemburger Strasse 116,
D-50939 Köln, Germany*

David Reguera

*Departament de Física Fonamental, Universitat de Barcelona, Martí i Franquès, 1,
08028 Barcelona, Spain*

Reinhard Strey

*Institut für Physikalische Chemie, Universität zu Köln, Luxemburger Strasse 116,
D-50939 Köln, Germany*

(Received 2 March 2007; accepted 1 June 2007; published online 8 August 2007)

We investigate the influence of carrier gas and thermostat on molecular dynamics (MD) simulations of nucleation. The task of keeping the temperature constant in MD simulations is not trivial and an inefficient thermalization may have a strong influence on the results. Different thermostating mechanisms have been proposed and used in the past. In particular, we analyze the efficiency of velocity rescaling, Nosé-Hoover, and a carrier gas (mimicking the experimental situation) by extensive MD simulations. Since nucleation is highly sensitive to temperature, one would expect that small variations in temperature might lead to differences in nucleation rates of up to several orders of magnitude. Surprisingly, the results indicate that the choice of the thermostating method in a simulation does not have—at least in the case of Lennard-Jones argon—a very significant influence on the nucleation rate. These findings are interpreted in the context of the classical theory of Feder *et al.* [Adv. Phys. **15**, 111 (1966)] by analyzing the temperature distribution of the nucleating clusters. We find that the distribution of cluster temperatures is non-Gaussian and that subcritically sized clusters are colder while postcritically sized clusters are warmer than the bath temperature. However, the *average* temperature of all clusters is found to be always higher than the bath temperature. © 2007 American Institute of Physics. [DOI: 10.1063/1.2752154]

I. INTRODUCTION

One of the simplest examples of a first-order phase transition is the condensation of a vapor into a liquid.¹⁻³ Like most first-order phase transitions, condensation starts through the mechanism of nucleation: first, a sufficiently large droplet or *nucleus* of the new phase must be formed by thermal fluctuations, which then can continue to grow to complete the phase transformation. The barrier towards nucleation arises from the energy cost this minute droplet has to pay to build its liquid surface in the vapor. Despite intense investigations for more than a century, nucleation is still elusive to an accurate quantitative description. For instance, recent experiments⁴⁻⁶ for the simplest case of condensation of argon vapor have revealed incredibly high deviations of more than 20 orders of magnitude from the still predominant classical nucleation theory.^{1,7,8}

Computer simulations have proven to be an invaluable resource to gain new insight into the subject at the molecular level. Probably the simplest, most-direct approach to simulate nucleation of a vapor on a computer is a standard or “brute-force” molecular dynamics (MD) simulation. Here, one simply starts from a homogeneous supersaturated vapor and follows the formation of the embryos of the liquid phase. The trajectories of the molecules are numerically calculated from the classical equations of motion while the particles interact through an intermolecular potential, which suits the

problem at hand—in the case of argon, typically the Lennard-Jones potential.^{9,10} The most frequently used ensemble for such a simulation method is the canonical NVT system, in contrast to most experiments, where we usually encounter (or much rather assume) μVT or NpT conditions. Nevertheless, results from simulations and experiment are still comparable as long as the system studied in the simulation is sufficiently large.¹¹

From a macroscopic point of view, the definition of temperature appears to be an obvious if not trivial task. However, in a small nonequilibrium system such as the clusters that are relevant in nucleation, the determination or even the definition of temperature is very subtle and not at all trivial. The main difficulty stems from the fact that during nucleation a significant amount of latent heat is released and the system thus surely is not in equilibrium. Consequently, it is clear that the old and the newly forming phase do not necessarily and in fact will not generally have the same (however well-defined) temperature. Furthermore, there is indeed some controversy surrounding the definition or even the application of the concept of temperature to small systems.¹²⁻¹⁶

Concerning nucleation, in particular, there have been many discussions on the role of the cluster temperatures and the influence of their inevitable fluctuations on the nucleation rate.¹⁷⁻²² The underlying idea is that the evaporation rate, the supersaturation of the vapor, and thus the nucleation rate (the

number of nuclei formed per unit time and volume) are very sensitive to even the slightest change in temperature. For that reason, both in experiment and in simulations, it is very important to keep the temperature of the system constant.

In experiments, quasi-isothermal conditions are achieved by diluting the condensable in an inert carrier gas that serves as a heat bath. This heat bath may then successfully absorb the latent heat that is released during condensation, provided that the excess of carrier gas is large and the nucleation rate sufficiently low. Nevertheless, various experiments have reported a so-called pressure-effect, where the nucleation rate depends on the pressure (and thus the amount) of the background carrier gas.^{23–25} The results are ambiguous, as are several theoretical approaches.

In computer simulations, and particularly in brute-force MD approaches, the problem is even more delicate. First, the attainable nucleation rates are extremely high, around $10^{24} \text{ cm}^{-3} \text{ s}^{-1}$ or higher. Consequently, the amount and the rate at which latent heat is released are much larger than in experiment. Second, the simulation of carrier gas to mimic the experimental solution is computationally not very appealing. The addition of a large number of carrier gas atoms will severely increase the computational cost. Therefore, a number of direct thermostating methods have been devised to avoid this problem, such as the simple velocity scaling scheme, the Andersen thermostat, or the Nosé-Hoover thermostat, all of which will be discussed in more detail below. These methods, especially the Nosé-Hoover thermostat, have been used extensively and usually perform the required task very well for equilibrium conditions.¹⁰ In nucleation, however, we face a two-phase system, which is not in equilibrium at all. The direct thermostats do not make distinctions between these two phases and also directly manipulate the condensed atoms in a way which may not resemble the physics of the underlying thermalization. For instance, the carrier gas atoms do not enter the center of a cluster.²⁶ Thus, the heat is only released from the cluster through collisions at or near the cluster surface, while the inner molecules only get cooled through subsequent internal collisions.

Despite these shortcomings and from a practical point of view, the question is how big the influence of the different thermostats on the resulting nucleation rate actually is. If the error is small, we may trade the physically more correct yet very expensive carrier gas simulation for a much faster direct method. Several publications have dealt at least partly with this question but none could in our view undoubtedly answer it.^{27–31} Moreover, the influence of temperature fluctuations and nonisothermal effects on the nucleation rate has long been discussed theoretically in the literature but, in our knowledge, never tested in a molecular simulation.

Therefore, our goal in this work was to perform a set of extensive MD simulations of nucleation of Lennard-Jones (LJ) vapor at two different supersaturations to answer these questions more thoroughly, aided by a newly developed method that accurately determines the nucleation rate (and more) from the simulation results.³² In particular, we will show how previously contradictory findings can be resolved

by carefully distinguishing between the bath temperature, the average cluster temperature, and the local equilibrium temperature of a cluster.

In the next section we will very briefly review the different direct thermostating methods used in this work focusing on their respective strengths and weaknesses rather than technical details, which can be found in excellent textbooks.^{9,10} In Sec. III we will describe the details of the performed MD simulations and the results are presented in Sec. IV. These results are analyzed in terms of the cluster temperatures and compared with the predictions of the classical work of Feder *et al.*³³ in Sec. V. Finally, the main conclusions are summarized in Sec. VI.

II. DIRECT THERMOSTATING METHODS

In this section, we briefly discuss the two direct thermostating methods used in this work.

A. Velocity scaling

The instantaneous (kinetic) temperature of a system is typically calculated from the mean kinetic energy per atom of the system, using the equipartition formula

$$\langle E_{\text{kin}} \rangle = \frac{1}{2N} \sum_{i=1}^N m_i v_i^2 = N_f kT/2, \quad (1)$$

where N_f is the number of degrees of freedom per molecule (three in the case of a simple atomic vapor such as argon), N is the total number of atoms, k is the Boltzmann constant, and T is the system temperature. In general, after one step (or many steps) of the dynamics, this instantaneous temperature will be different from the temperature of interest.

In the simple velocity scaling (VS) or isokinetic scheme, the instantaneous temperature of the system is adjusted to the desired temperature T_{set} by scaling all the velocities by a factor

$$v_{i,\text{new}}^2 = \frac{T_{\text{set}}}{T} v_i^2, \quad (2)$$

so that the mean kinetic energy of the total system after the rescaling coincides with the desired temperature of the system, i.e.,

$$\langle E_{\text{kin,new}} \rangle = \frac{1}{2N} \sum_{i=1}^N m_i v_{i,\text{new}}^2 = N_f kT_{\text{set}}/2. \quad (3)$$

If we perform this scaling in every time step in the simulation, we will rigorously force the temperature of the *entire system* to be equal to the target value T_{set} —at least for an equilibrium one-phase system. At the same time, however, this procedure has some serious drawbacks. First, temperature fluctuations that are natural also to the uniform canonical system are completely eliminated by this method. More importantly, we should bear in mind that this method does not in fact resemble a true canonical ensemble—it only yields the desired kinetic energy per particle for the system as a whole. On the plus side, this scheme is very fast and easily implemented in just a few lines of a code.

A different strategy is employed by the Andersen thermostat,³⁴ where instead of scaling the velocities of all atoms at once, one randomly picks one or a few atoms and draws their new velocity from a Boltzmann distribution at the desired temperature, thus mimicking a collision with a carrier gas particle. Nevertheless, we chose not to pursue a study of the Andersen thermostat on our nucleation simulations, since problems may occur when the thermostat randomly picks atoms of the core of a small cluster. The sudden change in velocity might actually break up or at least strongly destabilize such a cluster in a way that does not resemble the real physics of the process. In fact, a recent work using the Andersen thermostat reports that quantitative differences are found in the dynamics of the decay of small LJ clusters.³⁵

B. The Nosé-Hoover thermostat

Arguably, the most popular technique for MD simulations at a constant temperature (or pressure) is the Nosé-Hoover thermostat. Nosé introduced an additional coordinate, which is associated with an effective “mass” Q and enters as an additional “friction” term into the laws of motion, corresponding to an extended Lagrangian method.^{36,37} This additional constraint may keep the temperature (or pressure) constant. Hoover later showed that the Nosé equations of motion could be simplified in a way that is simpler to implement in a code in terms of real variables. In addition, he pointed out that this set of equations is unique in the sense that any other set of equations does not yield the correct canonical ensemble.^{38,39} Implementations of these equations are commonly referred to as the Nosé-Hoover (NH) thermostat. The NH thermostat does conserve a canonical ensemble and allows the temperature to fluctuate realistically.

Simply put, the Nosé-Hoover thermostat changes the particle velocities to the desired value more gradually and smoothly, instead of the instantaneous changes in the VS or Andersen thermostat. The coupling to the imaginary heat bath can be controlled by the effective mass Q . A strong coupling quickly adjusts the system temperature at the expense of quite large and rapid fluctuations, while a weak coupling does the same job more smoothly. In the limit of a very weak coupling, it yields an NVE rather than an NVT ensemble. The Nosé-Hoover thermostat correctly preserves the canonical ensemble and the fluctuations in the system temperature, but at the expense of being more time consuming in the simulation. Typically, an iterative algorithm is employed,⁴⁰ with each iteration taking roughly as long as one simple velocity scaling step, so that the calculation time considerably increases when many iterations are necessary. In addition, there is no exact way to determine a “correct” or appropriate coupling constant Q for the system *a priori*. It remains a free parameter that can and has to be adjusted based on a combination of an educated guess, experience, and trial and error (see also, e.g., Appendix B of Ref. 41).

III. MOLECULAR DYNAMICS SIMULATIONS

A. Details of the simulations

In order to investigate the influence of the different thermostats on the nucleation rate, we performed molecular dynamics simulations of Lennard-Jones atoms in a cubic box with periodic boundary conditions using a velocity-Verlet algorithm.^{9,10} We chose to perform simulations of argon at 50 K, inside the same temperature range reported by Fladler and Strey⁴ and Iland^{5,6} in their recent experiments. The number of LJ argon atoms was fixed at $N=343$ in all simulations, which is sufficiently large without encountering significant finite-size effects.¹¹ Two different box volumes, $V=(16\text{ nm})^3$ and $(18\text{ nm})^3$, were chosen corresponding to a high supersaturation (low nucleation barrier) and a low supersaturation (high nucleation barrier), respectively. The argon parameters for the LJ potential were taken as $\sigma=0.3405\text{ nm}$ and $\varepsilon/k=120\text{ K}$, and the time step was 2 fs. The potential was not shifted but truncated at $r_{\text{cut}}=5\sigma$. The liquid clusters forming in the system were identified using a simple Stillinger criterion with a threshold distance of $r_c=1.8\sigma$. The simulation program was largely based on the program CLUSTER developed by Wonczak and used in Refs. 28 and 42.

Three different thermostating methods were used in the simulation. In a first set, velocity scaling (VS) was performed at every time step.

In the second set, the NH thermostat was used,^{41,40} where in the initial time step the velocities are rescaled to the desired temperature and the center of mass movement of the system is set to zero. We made several tests with different values of the coupling constant Q in the range of $Q=0.1-13\,000$ and found only very small deviations in the results. Therefore, we chose a value of $Q=2$ for the remainder of the work, corresponding to the typical choice suggested in the literature.^{36,41,40} The maximum deviation for different values of Q was less than 15% in the rate and less than 2% in the critical size (for the analysis see next section). For the high barrier system, $V=(18\text{ nm})^3$, the difference between VS and NH was almost nonexistent.

Finally, we repeated the simulations at the same conditions with three different ratios of vapor to carrier gas of roughly 1:1, 1:2, and 1:3. In the carrier gas simulations, LJ helium atoms, with parameters $\sigma_{\text{He}}=0.258\text{ nm}$ and $\varepsilon_{\text{He}}/k=10.22\text{ K}$, are added and only these atoms are subjected to a VS thermostat. The standard Lorentz-Berthelot mixing rules are used to set the interaction parameters between helium and argon atoms.

For most simulations, we used standard PC hardware (Intel Pentium IV at 3.2 GHz) and the run times of simulations were on the scale of a few minutes for the systems without carrier gas and velocity scaling and up to 1 week for the largest system with carrier gas. The simulated time was up to 2000 ns or equivalently 10^9 time steps. Each particular set of simulations was repeated many times to achieve good statistics. First, the vapor phase was equilibrated at $T=100\text{ K}$ for 20 ns. Then, we captured up to 1000 different configurations, equally spaced at 20 ps intervals, from this homogeneous vapor phase. Each of these configurations then

TABLE I. The supersaturation S , equilibrium vapor pressure p_{eq} at 50 K (Ref. 50), nucleation time τ_J , nucleation rate J , ratio of the rate J over the rate of the system with the velocity scaling thermostat J/J_{vs} and critical cluster size n^* for each thermostat.

Property/ units thermostat	No. of sim.	S	p_{eq} (Pa)	τ_J (ns)	J ($10^{24} \text{ cm}^{-3} \text{ s}^{-1}$)	J/J_{vs}	n^*
Velocity scaling	1000	869	66.5	22.3	10.9	1.0	13.2
Nosé-Hoover	300			20.7	11.8	1.1	13.7
386 He	300			20.2	12.1	1.1	12.8
657 He	300			15.6	15.7	1.4	12.8
988 He	300			12.9	18.9	1.7	12.5
Velocity scaling	300	610	66.5	321	0.53	1.0	14.1
Nosé-Hoover	200			337	0.51	1.0	13.9
386 He	300			296	0.58	1.1	14.1
657 He	300			226	0.76	1.4	14.0
988 He	300			211	0.81	1.4	13.8

served as a unique starting point and was subjected to an instantaneous temperature jump to $T=50$ K. In each simulation, we monitor the largest cluster forming in the system. All simulations were aborted when this largest cluster in the system exceeded a size of $n=55$ for at least 20 ps. Table I shows the number of simulation runs performed under each condition. Overall, almost 4000 systems were simulated for the present study.

Instead of simulating one large system with many nucleation events, we performed many simulation runs of a small system, where predominantly only one event occurs. This procedure has several advantages. First, for a large system we would need a very high supersaturation to observe many nuclei and get a good statistics. These clusters, however, certainly do not form at the same time but subsequently under very different conditions, because the vapor phase will rapidly decrease in a canonical system as more and more nuclei appear.¹¹ Second, a simulation of a smaller system with only one nucleation event repeated several times runs faster on a computer than one large-scale simulation with effectively the same number of nucleation events.

Typically, Lennard-Jones simulation data are reported in reduced units. However, we chose to report our results in standard SI units instead to facilitate the direct comparison with experiments and to make the work more accessible to experimentalists working in the field.

B. Mean first-passage time analysis of the nucleation rates

We analyzed the simulation data using the recently introduced mean first-passage time method.³² This method offers a very efficient, easy-to-implement, and rigorous procedure to evaluate nucleation rates in MD simulations. The idea is very simple: for each system we note the first-passage (or appearance) time $t(n)$, which is the time when the *largest cluster* reaches or exceeds the size n for the *first* time. This is done for all simulation runs of one system and the average yields the mean first-passage time (MFPT) $\tau(n)$ as a function of n . It is important to note that this $\tau(n)$ is the MFPT of the *whole* system. It does not matter which particular cluster

reaches or exceeds n for the first time, only that the system as a whole exhibits any one cluster of that given size.

The MFPT is related to the nucleation rate in a very simple way. For a reasonably high nucleation barrier, the MFPT as a function of the size of the cluster in the vicinities of the critical cluster size is given by the following expression:³²

$$\tau(n) = \frac{\tau_J}{2} [1 + \text{erf}((n - n^*)c)], \quad (4)$$

where n^* is the size of the critical cluster, $\text{erf}(z)$ is the error function,

$$c = \sqrt{\frac{|\Delta G''(n^*)|}{2kT}} = \sqrt{\pi}Z \quad (5)$$

is connected to the so-called Zeldovich factor Z [$\Delta G''(n^*)$ being the value of the second derivative of the free energy of formation at the critical cluster size], and τ_J is the nucleation time, which is related to the nucleation rate J by

$$J = \frac{1}{\tau_J V}. \quad (6)$$

Therefore, by a simple three-parameter fit of the simulation results to Eq. (4), we immediately get all the relevant quantities of the nucleation process. Here, we will only be interested in the change of the actual nucleation *rate*. A more thorough discussion of the method and the relevance of the other two parameters can be found in Ref. 32.

Figure 1 shows the results of the MFPT corresponding to the MD simulations using the different thermostating methods for a high [Fig. 1(a)] and a low supersaturation [Fig. 1(b)]. Table I gives an overview of the resulting nucleation times and nucleation rates. Figure 1(b) shows that expression (4) fits the MD results very well. However, the MFPTs in Fig. 1(a) do not truly lead into a plateau as the fit does. This indicates a regime where the nucleation barrier is very low and nucleation and growth occur on similar time scales. As discussed in Ref. 32, an alternative definition of the nucleation time valid for this low barrier case would be twice the

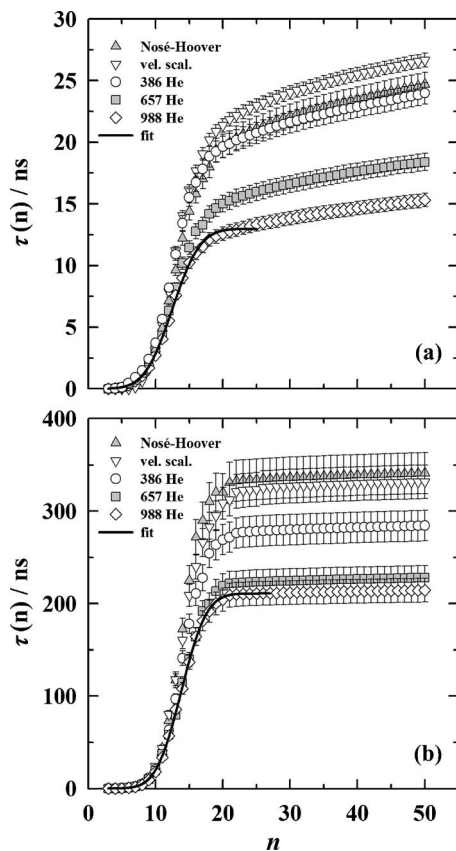


FIG. 1. (a) Mean first-passage times of the largest nucleating cluster in a system of $N=343$ argon atoms in a volume of $V=(16 \text{ nm})^3$ and a temperature $T=50 \text{ K}$ ($S=869$), which is held constant by velocity scaling, a Nosé-Hoover thermostat, or three different amounts of a helium carrier gas. (b) Same as for a system volume of $V=(18 \text{ nm})^3$ ($S=610$).

time at the inflection point of the MFPT curve. However, it was also shown that the differences are very small and unimportant in this case.

IV. RESULTS

A. Nucleation rates

Since in both Figs. 1(a) and 1(b) the volumes are fixed for all systems, we can easily infer how the rate changes: it is just the inverse of the nucleation time. We see in both cases that the nucleation rate is lowest (i.e., the nucleation time is larger) when using direct thermostats, either NH or VS, followed by the simulations with carrier gas. In addition, the nucleation rate increases with increasing amount of carrier gas. This behavior is similar for both the high and the low supersaturation but less pronounced in the latter case, where it seems that the addition of more carrier gas beyond a 1:2 ratio does not change significantly the rate. Moreover, the choice of the direct thermostat does not influence the rate at all in this case.

The results compiled in Table I also summarize the deviation of the nucleation rate with respect to the simplest and fastest thermostating method, namely, velocity scaling. Quite surprisingly, the deviations are much smaller than one would have naively expected, considering the length and depth of discussions in the literature about possible effects related to nonisothermal effects and temperature fluctuations. The dif-

ference in nucleation rates never exceeds a factor of 1.7, which can be considered as negligible in nucleation, where discrepancies reaching several orders of magnitude are typical and common. For example, in the two-valve nucleation pulse chamber, the standard error in the nucleation rate is reported as a factor of two.⁴³ Moreover, in many cases the results of measurements of nucleation rates of the same substance at the same conditions but using different experimental techniques can disagree by several orders of magnitude.

B. Average cluster temperatures

In addition to the rate, we have analyzed the “temperature” of the growing clusters. As mentioned in the Introduction, it is not trivial to define what the temperature of clusters consisting of a few tens of atoms or less actually is. In our case, we will focus on the kinetic temperature of a cluster of n molecules, calculated from its mean kinetic energy as

$$\frac{3}{2}kT(n) = \frac{1}{2n} \sum_{i=1}^n m_i v_i^2. \quad (7)$$

It is not obvious that this instantaneous definition of temperature corresponds to the “real” cluster temperature, since the concept of temperature becomes controversial for very small and out of equilibrium systems such as the clusters we are interested in. In addition, we do not take into account the possible interplay of translational, rotational, or vibrational degrees of freedom of the growing clusters. Still, if we average over a sufficiently high number of incarnations of a cluster at one size n , we can expect that this kinetic temperature will provide a reasonable estimate of the true temperature. It might in fact well be the best possible choice to measure the temperature for such a small, nonequilibrium system.⁴⁴

Let us start by determining and discussing the average cluster temperatures. The average temperature of a cluster of a given size is calculated in the following way. In each simulation run, we look at the largest nucleating cluster and its size n . For this cluster, we note its instantaneous temperature. This information is taken every 0.2 ps for each simulation. We then average this instantaneous temperature for each size over all simulations of one system, thus obtaining the average cluster temperature $T_{\text{avg}}(n)$ as a function of its size n . The number of snapshots we obtain for each size n in each set of simulation runs is quite large and in the range of 10^4 – 10^6 configurations.

Figure 2(a) shows the temperature difference ΔT between the average cluster temperature T_{avg} (filled symbols) and the imposed bath temperature of 50 K as a function of the cluster size n using the different thermostats for the case of a high supersaturation [Fig. 1(a)]. Values smaller than $n=6$ are not reported for two main reasons: poor and biased statistics. This is because, as stated above, only the largest cluster in the system is monitored. Due to thermal fluctuations, clusters of sizes smaller than 5 are almost always present in the system, and not being the largest, they are not monitored (sampled) in our simulation.

From the results, we first notice the expected behavior that the growing cluster heats up due to the release of latent

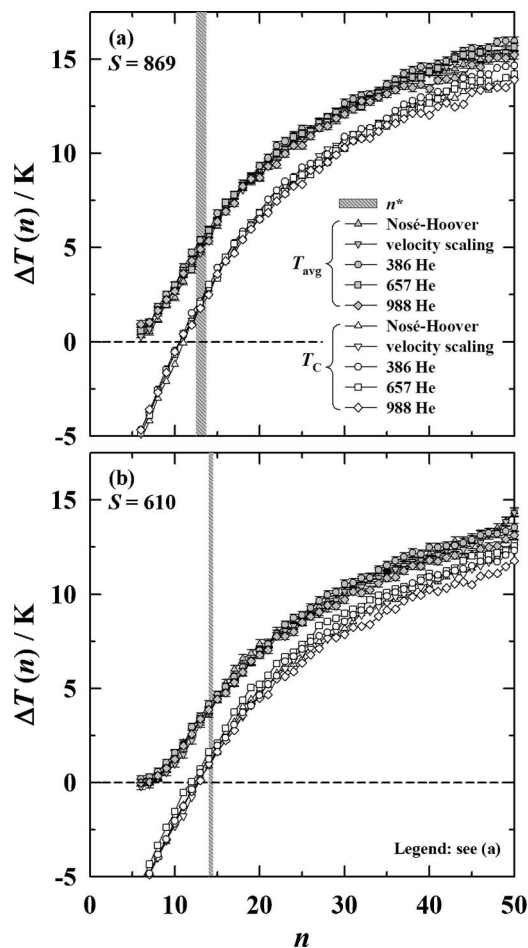


FIG. 2. Deviation of the average cluster temperatures (filled symbols) T_{avg} and local equilibrium cluster temperature T_c from the desired bath temperature of 50 K as a function of the cluster size n : (a) for $S=869$ [$V=(16 \text{ nm}^3)$] and (b) for $S=610$ [$V=(18 \text{ nm}^3)$].

heat from the condensation. In addition, note that this average temperature of clusters is always higher than the fixed bath temperature of 50 K. Quite surprisingly, however, it turns out that there is no noticeable difference in the average cluster temperatures for all the different thermostating techniques that we have used in this work.

Figure 2(b) shows the results for the low supersaturation (i.e., high nucleation barrier) case [corresponding to the MFPTs of Fig. 1(b)]. We find the same qualitative picture, but the shift in temperatures with respect to the bath temperature is less pronounced than in the low barrier case. Note also that for a given size the cluster temperature is higher in the high supersaturation situation because the clusters grow faster and have less time to thermalize than in the low supersaturation case.

There is a very important point that might appear puzzling at first glance: even for the strict velocity scaling scheme, the temperature of the clusters *does not* in general coincide with the imposed bath temperature of 50 K. It is worth stressing that the only quantity that is kept constant by the velocity scaling thermostat is the desired kinetic energy per particle for the entire system. However, if we measure the instantaneous temperature of a cluster of n molecules via their kinetic energy, this temperature does not in general co-

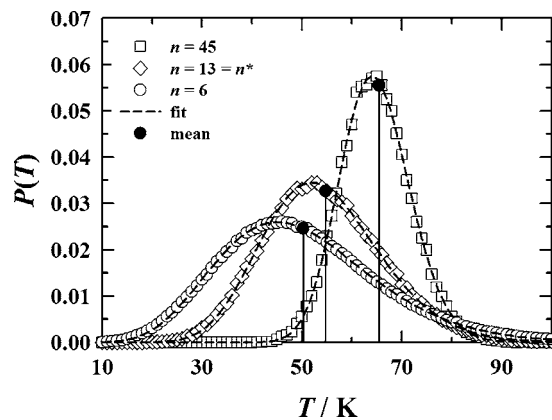


FIG. 3. Cluster temperature distribution for subcritically, critically, and postcritically sized clusters, taken from the simulations with $S=869$ [$V=(16 \text{ nm}^3)$] and velocity scaling. For small cluster sizes, the distribution is non-Gaussian. The distributions can be very well described by a fit to Eq. (10).

incide with the global bath temperature. Moreover, the temperature of this cluster will fluctuate strongly due to the continuous change in its composition from successive evaporation/condensation events. Such a temperature fluctuation is inevitable—despite the fact that velocity scaling keeps (at every time step) the global temperature of the entire system strictly constant. As we will see in Sec. V, these temperature fluctuations and the net shift of the average temperature arise from the heat released from the condensation/evaporation of molecules during nucleation.

C. Cluster temperature distributions: The local equilibrium cluster temperature

In addition to the average temperature, a lot of information can be gained by looking at the full temperature distribution of clusters of each particular size. Figure 3 shows the distribution of cluster temperatures for three different cluster sizes, corresponding to subcritical, critical, and postcritical cluster sizes. These example distributions were taken from the simulations with velocity scaling and a high supersaturation.

The cluster temperature fluctuates over a wide range of values. In addition, the temperature distribution is clearly not Gaussian for critically sized or smaller clusters. In this case, the average temperature of a cluster will not be a good measure of the most likely temperature of clusters of that size, i.e., the peak of the temperature distribution $T_c(n)$.

The distribution of equilibrium temperature fluctuations for a small system (in our case, a small cluster of a given size) around a given “bath temperature” T_0 was given by McGraw and Laviolette:¹⁸

$$P(T) = K_1 \exp(-W(T)/kT_0), \quad (8)$$

where K_1 is a normalization constant and $W(T)$ is the reversible work required to bring the system from its equilibrium temperature T_0 to a temperature T :

$$W(T) = C_V(T - T_0) + C_V T_0 \ln(T_0/T), \quad (9)$$

where C_V is the heat capacity of the liquid clusters.

These equations describe the equilibrium fluctuations of a small cluster of a fixed size around its equilibrium temperature T_0 . It is, however, important to bear in mind that the nucleating clusters are *not* at equilibrium and hence, their temperature might not coincide in general with the (global) bath temperature, e.g., 50 K in our case.

The release/intake of latent heat as a consequence of the fact that the clusters are growing and shrinking in size leads to a net shift in the temperature of the clusters. Between successive condensation/evaporation events, the clusters have a comparatively long lifetime that allows them to equilibrate their local temperature.²² Hence, at steady-state conditions an ensemble of clusters of a particular size will be locally equilibrated around this shifted temperature.

It is a reasonable assumption—consistent with the ideas of nonequilibrium thermodynamics—that the distribution of fluctuations around this shifted (or local equilibrium) temperature will have the same functional form as around the true equilibrium conditions. It will thus be described by an equation similar to Eqs. (8) and (9), namely,

$$P(T) = K_1 \exp(- (C_V(T - T_C) + C_V T_C \ln(T_C/T))/kT_C), \quad (10)$$

where T_C now is the *local* equilibrium temperature of the cluster, which plays the same role as T_0 for an equilibrium system.

We can use Eq. (10) to fit the temperature distributions in Fig. 3, using the cluster temperature T_C and the heat capacity C_V as free parameters. The fit is also plotted in the same figure, yielding excellent agreement with the simulation results. We repeated this procedure for all cluster sizes in all simulated systems. Figure 2 shows the resulting cluster temperatures T_C as a function of the cluster size n . The important difference to the average cluster temperatures is that the temperature of clusters smaller than the critical size is most likely *below* the enforced bath temperature of 50 K.

Therefore, the average temperature T_{avg} of the cluster is always higher than that of the bath, while the local equilibrium temperature T_C , i.e., the peak of the distribution of temperature fluctuations, is lower than the bath temperature for clusters smaller than the critical size and larger for postcritically sized clusters.

This subtle result in fact clarifies the apparently contradictory results of different previous treatments of nonisothermal effects, which disagreed upon whether the temperature of subcritical clusters were higher or lower than the bath temperature. The origin of the discrepancy may lie in whether the average or the local equilibrium temperature was considered. Finally, we also note that for larger clusters the distribution of temperatures is gradually becoming more and more Gaussian, also in agreement with theoretical predictions.

In Figs. 4(a) and 4(b), the second fitting parameter, namely, the heat capacity of the cluster, is given as a function of the cluster size in units of the Boltzmann constant k . We note that the slope of the curve is quite close to 1.5 and hence the heat capacity per molecule is almost equal to the ideal value of $(3/2)k$ quite independently of the chosen thermostatting method. However, the results from velocity scal-

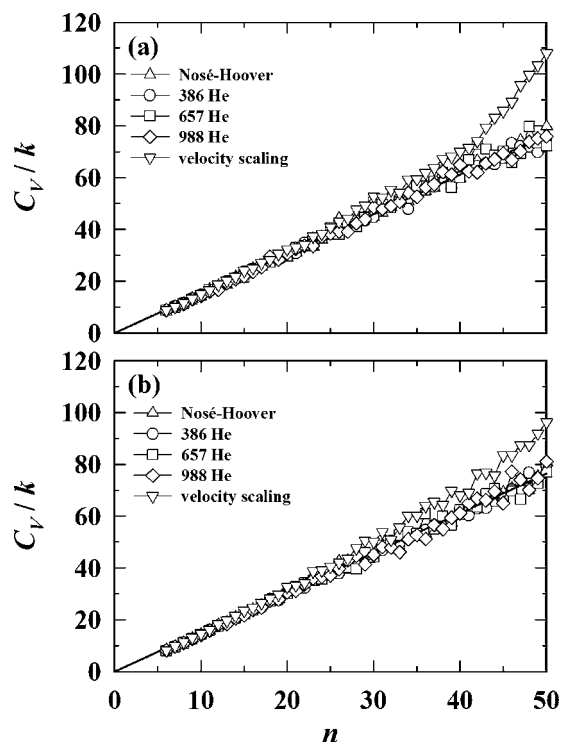


FIG. 4. Heat capacity C_V of clusters in units of the Boltzmann constant k as a function of the cluster size n for the conditions (a) $S=869$ and (b) $S=610$.

ing in Fig. 4 already indicate that this kind of thermostat might become less and less appropriate as the clusters grow. One typical artifact of the VS thermostat [possibly also of the NH thermostat (Ref. 45)] we encounter when we let the cluster fully condense in the system is that instead of a liquid drop, we might end up with a crystal-like structure with fixed atoms which is not translating at all but rotating at very high speeds.

An analysis of the obtained results in the light of the classical nonisothermal nucleation theory work of Feder *et al.*³³ is described in the following section.

V. COMPARISON TO CLASSICAL NONISOTHERMAL NUCLEATION THEORY

A. The influence of the carrier gas

There have been several studies dealing with the role of nonisothermal effects and temperature fluctuations on nucleation rates.^{17–21} These studies have reported different and often contradictory predictions of the temperature of a nucleating and growing cluster and its influence on the nucleation rate. Yet to our knowledge, the validity of these predictions has never been tested in a molecular simulation, although numerical algorithms solving the energy and mass balance of clusters have been reported.^{18,20} Our precise evaluation of nucleation rates by the MFPT method opens up the possibility of a quantitative test of the predictions of the different theories and the importance of nonisothermal effects.

Among all theories, the classical work of Feder *et al.*³³ offers simple analytical expressions to quantify the influence of nonisothermal effects on the nucleation rate and the cluster temperatures, and we will see that it provides a remark-

able semiquantitative agreement with the data. Feder *et al.* studied the effect of the released latent heat in the nucleation process by analyzing the evolution of clusters both in size and in energy. Using irreversible thermodynamics, they obtained very simple expressions for both the temperature of the clusters and the nonisothermal rate in terms of two quantities that control the importance of thermal effects, q and b . The parameter

$$q = h - \frac{kT_0}{2} - \gamma \frac{\partial A(n)}{\partial n} \quad (11)$$

quantifies the energy released when a monomer is added to a cluster, which basically is the latent heat h per molecule corrected by a small amount $kT_0/2$ (the excess of energy of a colliding molecule) minus the energy $\gamma[\partial A(n)/\partial n]$ spent in increasing the surface area $A(n)$ against the surface tension γ upon the addition of a molecule.

The term

$$b^2 = (c_V + \frac{1}{2}k)kT_0^2 + \frac{\beta_c}{\beta}(c_V^c + \frac{1}{2}k)kT_0^2 \quad (12)$$

is the mean squared energy fluctuation between two evaporation/condensation events removed by collisions with impinging vapor (the first term on the right hand side) and carrier gas (the second term on the right hand side) molecules.

In the previous equation, c_V is the specific heat capacity per molecule of the condensable vapor, and c_V^c is the specific heat capacity per molecule of the carrier gas; $\beta = p/\sqrt{2\pi mkT_0}$ and $\beta_c = p_c/\sqrt{2\pi m_c kT_0}$ are the frequencies of collisions with vapor and carrier gas molecules, respectively; m and m_c are the mass of a molecule of the vapor and carrier gas, respectively; p and p_c are their corresponding pressures.

Physically, the importance of the nonisothermal effects is controlled by the ratio of q and b —the ratio between the energy increase due to the release of latent heat and the (root mean squared) energy carried away by collisions with both vapor and carrier gas molecules. In classical nucleation theory (CNT), it is assumed that every molecule that collides with a cluster will attach to it but here we could also take into account an accommodation coefficient different from 1. Note also that, in the absence of a carrier gas, q/b has a finite value that can be big, so that the system will only be poorly thermalized.

In terms of these two quantities, the prediction for the nonisothermal steady-state nucleation rate is³³

$$J_{\text{noniso}} = \frac{b^2}{b^2 + q^2} J_{\text{iso}}, \quad (13)$$

and the temperature shift $\Delta T = T_C - T_0$ of the temperature T_C of a cluster of size n with respect to the bath temperature T_0 is given by

$$\Delta T = T_0 \frac{q}{b^2 + q^2} \left(- \frac{\partial \Delta G(n)}{\partial n} \right), \quad (14)$$

where $\Delta G(n)$ is the free energy of formation of a cluster of size n . In the classical approximation, this free energy is given by $\Delta G(n) = -nkT \ln S + \gamma A(n)$, where S is the super-

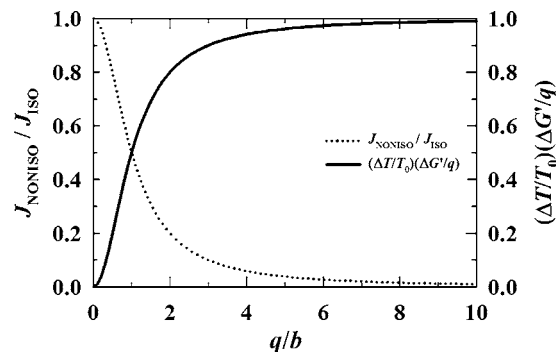


FIG. 5. Dependence of the nonisothermal nucleation rate and the normalized temperature shift according to classical nonisothermal nucleation theory as a function of the ratio q/b .

saturation. Therefore, the temperature shift is proportional to the derivative of the free energy of formation, and hence, clusters smaller than the critical size are predicted to be colder than the bath, and clusters bigger than the critical size will be warmer, just as we have found in the simulations.

The behavior of the rate and the normalized temperature shift as a function of the ratio q/b is plotted in Fig. 5. In the limit of a very efficient thermalization (i.e., $q/b \rightarrow 0$), the rate tends to the isothermal value and clusters of all sizes will have the temperature of the bath. As q/b increases, the rate decreases, and the magnitude of the temperature shift increases. Note that the nonisothermal rates are only slightly smaller than the isothermal ones, despite the fact that the temperature of the clusters can be several degrees higher than that of the bath.

We can now test these simple predictions against the results of our MD simulations. For an ideal monatomic vapor and carrier gas, $c_V = c_V^c = (3/2)k$, and the expression for b^2 simplifies to

$$b^2 = 2k^2 T_0^2 \left(1 + \frac{N_c}{N} \sqrt{\frac{m}{m_c}} \right), \quad (15)$$

which indicates that a large number of carrier gas molecules N_c and a light carrier gas (i.e., a small m_c) are more effective in achieving a good and fast thermalization. This latter point is rather counterintuitive at first sight, as one would imagine that big and heavy atoms would serve as a better heat reservoir. In fact, however, the smaller and lighter atoms yield a much higher collision frequency and, as a net result, can carry away a larger amount of energy through many more collisions than bigger and heavier atoms.

Figures 6(a) and 6(b) plot the prediction for the temperature shift of the clusters as a function of its size for different values of the ratio N_c/N for both the low and high supersaturation cases. The latent heat of argon is obtained from the equilibrium vapor pressure using the Clausius-Clapeyron equation. The thermophysical properties of argon used in CNT are listed in Table I of Ref. 8. Despite the fact that we are using CNT—whose predictions are expected to be inaccurate—to calculate the temperatures, the predictions agree surprisingly well with the results obtained from the MD simulations (see Fig. 2).

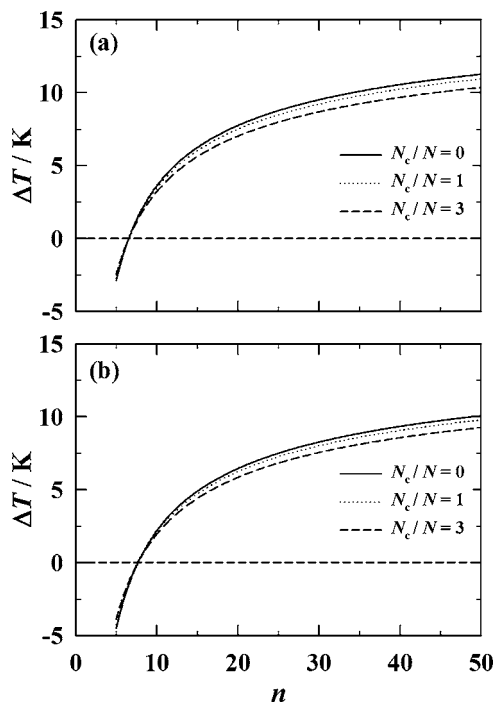


FIG. 6. Cluster temperature differences according to classical nonisothermal nucleation theory as a function of its size, for different values of N_c/N , the ratio of carrier gas to condensable molecules: (a) for $S=869$ and (b) for $S=610$.

Although cluster temperatures are several degrees different from the bath temperatures, the influence of the nonisothermal effects on the nucleation rate are not that strong. Figure 7(a) plots the predicted influence of the ratio of carrier gas to condensable molecules, N_c/N , on the nucleation rate for the case of argon at 50 K using helium as a carrier gas. Figure 7(b) shows the same plot, where the deviation is being referred to its value at a ratio $N_c/N=1$, thus enabling us to include the results from the simulations. The numerical values are amazingly close to the values obtained in the simulations. One can also observe that in the complete absence of carrier gas, the rate can be around a couple of orders of magnitude smaller than in a system that is well thermalized. Since most experiments are typically performed with a large excess of carrier gas, they can be expected to be very well thermalized. Here, however, we can already see that a 3:1 carrier gas to vapor ratio is probably not sufficient to measure a truly isothermal rate.

B. The influence of direct thermostats

The fact that the rates obtained with VS and NH thermostats are slightly lower than with a carrier gas seems to indicate that they are less efficient in achieving a proper thermalization of the nucleating clusters. This finding appears quite counterintuitive at first glance, since one would assume that direct methods, and especially the strict velocity scaling, would rigorously enforce the desired temperature. In the following, however, we will see that this finding is perfectly reasonable.

It is not quite as straightforward to perform a quantitative evaluation of the effectiveness of direct thermostats as

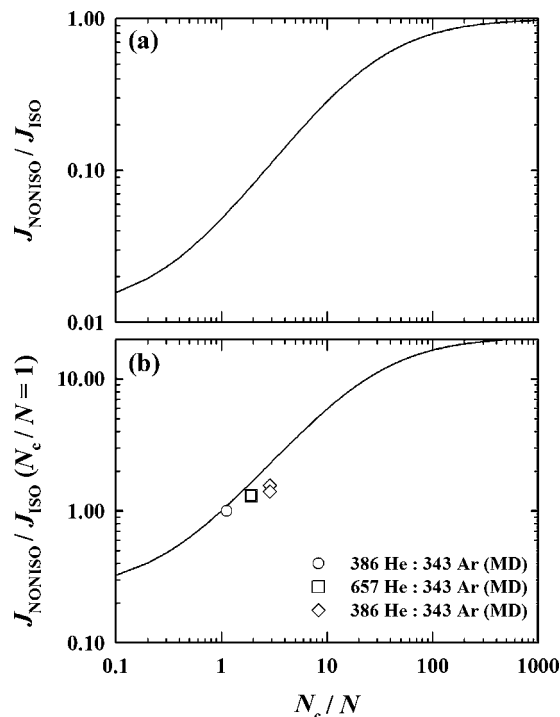


FIG. 7. (a) Dependence of the nonisothermal nucleation rate according to classical nonisothermal nucleation theory on the ratio N_c/N of carrier gas to condensable molecules. (b) Ratio between the nonisothermal nucleation rate referred to its value at a ratio $N_c/N=1$, as a function of N_c/N . Data points are the simulation results.

was done in Sec. II A for the case of a carrier gas. Nevertheless, we can assimilate the effect of the direct thermostating on a cluster to a sort of effective collision that changes its energy and thus make an order of magnitude estimate of what will be the contribution of a direct thermostat to the value of b^2 . As it was mentioned before, the “energy diffusivity” b^2 gives a measure of the energy change between two successive condensation/evaporation events. There is always a contribution to b^2 due to collisions with vapor molecules [the first term on the right hand side of Eq. (12)], and in the presence of a carrier gas, there is another contribution due to collisions with carrier gas molecules [the second term on the right hand side of Eq. (12)]. To estimate the contribution of the direct thermostats to b^2 , we have to evaluate the typical amount of energy removed from the cluster by the direct thermostat between two condensation/evaporation events. An estimate of the typical energy change per molecule that occurs in the simulation in a given time step would be the typical force times the typical displacement of the atoms in the given time step, namely,

$$\Delta E_{VS} \sim \frac{1}{2}F\Delta x \sim \frac{1}{2}\frac{\varepsilon}{\sigma}v\Delta t \sim \frac{1}{2}\frac{\varepsilon}{\sigma}\sqrt{\frac{kT}{m}}\Delta t, \quad (16)$$

where F denotes the order of magnitude of the force (that for a LJ potential is given by ε/σ) and $\Delta x \sim v\Delta t$ the typical displacement in Δt , v being the thermal velocity.

Therefore, the average change in energy squared per molecule and unit time would be

$$\frac{(\Delta E_{\text{VS}})^2}{\Delta t} \sim \frac{1}{4} \left(\frac{\varepsilon}{\sigma} \right)^2 \frac{kT}{m} \Delta t. \quad (17)$$

If we are considering a cluster of n molecules, the average change in its energy squared due to the thermostat in the time between two successive attachment or detachment events is

$$\frac{(n\Delta E_{\text{VS}})^2}{\Delta t} \frac{1}{\beta A(n)} = \frac{1}{4} \left(\frac{\varepsilon}{\sigma} \right)^2 \frac{kT}{m} \Delta t \frac{n^2}{\beta A(n)}, \quad (18)$$

where $1/\beta A(n)$ is the time between two condensation/evaporation events (i.e., the inverse of the frequency of collision). Therefore we can translate the average change in energy due to the thermostat to an effective contribution to b^2 of roughly

$$\Delta b_{\text{VS}}^2 \sim \frac{(n\Delta E_{\text{VS}})^2}{\Delta t} \frac{1}{\beta A(n)} = \frac{1}{4} \left(\frac{\varepsilon}{\sigma} \right)^2 \frac{kT}{m} \Delta t \frac{n^2}{\beta A(n)}. \quad (19)$$

For instance, if we use VS and readjust the energy after every time step Δt (2 fs in our case), we get for an argon cluster of $n=14$ (approximately the critical cluster size) a contribution of roughly

$$\Delta b_{\text{VS}}^2 \sim 4(kT)^2. \quad (20)$$

We can compare this value with the contribution that would arise from a hypothetical amount of helium carrier gas, i.e., $\Delta b_{\text{carrier}}^2 = (N_c/N) \sqrt{(m/m_c)} 2(kT)^2$. The value of $4(kT)^2$ given by Eq. (20) is equivalent to have a $N_c/N=0.7$ helium carrier gas mixture. Hence, we can expect that rescaling the velocities even at every time step has roughly a similar efficiency than a 1:1 helium carrier gas mixture.

This finding is also consistent with the results of our MD simulations. In fact, our estimate is expected to be an upper bound. For example, for the pure vapor at 50 K, we find from the simulations that the average energy removal per particle (squared) from a velocity scaling thermostat to be only $1.5 \times 10^{-8}(kT)^2$ per molecule and time step compared to $5 \times 10^{-7}(kT)^2$ from Eq. (17). In fact, significant changes in the energy of the molecules are only expected for the few molecules that constitute the cluster. However, the energy change from the thermostat will then be shared among *all* the molecules in the system—not just those up-heating atoms of the cluster. Indeed, for that reason one can expect that this type of thermostat would even be less efficient for a higher total number of molecules in the system. We have already simulated large systems at the same density and have found the expected behavior, i.e., a slightly decreasing rate with an increasing total number of atoms.¹¹ Finally, one would expect that NH, readjusting the temperature in a smoother way, cannot be significantly more efficient in thermalizing the system compared to VS, as we find in the simulations.

Quite intriguingly, Eqs. (16) and (19) suggest another possibility to increase the efficiency of a direct thermostat. Since the typical energy removal is proportional to Δt , it suggests that a longer time step or a less frequent rescaling would result in a more effective cooling (obviously, this scaling is only valid for small Δt). Especially the latter suggestion again might be quite counterintuitive at first glance. Consequently, we have investigated the influence of the time

TABLE II. The nucleation rate J and critical cluster size n^* for different values of the simulation time step Δt , and the frequency of rescaling f_{VS} (the inverse giving the number of time steps after which all velocities are rescaled). All results are obtained using velocity rescaling and are based on 200 simulations at the same conditions as the reference point from Table I which is based on 1000 simulations.

Δt (fs)	$1/f_{\text{VS}}$	$\Delta t/f_{\text{VS}}$ (fs)	J ($10^{24} \text{ cm}^{-3} \text{ s}^{-1}$)	n^*
2	1	2	10.9	13.2
5	1	5	13.6	12.4
10	1	10	17.0	11.8
20	1	20	24.8	10.3
2	5	10	14.9	12.6
2	10	20	24.0	11.7
2	100	200	70.2	10.1
2	1000	2000	32.5	11.7

step length Δt and the rescaling frequency f_{VS} on the nucleation rate using VS for the case of $V=(16 \text{ nm})^3$. The results are compiled in Table II. Exactly as predicted, the rate increases with increasing time step. The rate also increases when we rescale the velocities of all particles less frequently than in every time step. Moreover, at the same ratio of $\Delta t/f_{\text{VS}}$ we get very similar rates. Hence, we find that a less frequent rescaling and a longer time step greatly improve the efficiency of VS in removing the latent heat from the nucleating system. However, one cannot push this idea too far and should proceed with caution in the choice of these parameters. On the one hand, the increase in time step is limited and should not be pushed beyond a limit that still yields physically reasonable trajectories of the particles. On the other hand, the result for $1/f_{\text{VS}}=1000$ already indicates that if the rescaling is too infrequent the rate goes down again; in this case the system is evolving nonisothermally for quite a long time between the rescaling events.

The true origin of the difficulty of the direct methods to cool a condensing cluster even more effectively is of course their inability to distinguish between the gas and the liquid cluster in the simulation—all atoms are treated equally, no matter which state or which temperature they have. Naturally, one is inclined to devise a method that would first identify the cluster and then treat these atoms differently from the remaining gas molecules. However, this procedure would face many difficulties, especially for small clusters. One of them is related to the ambiguities in the proper definition of a cluster. While the Stillinger definition gives a good measure and is sufficiently accurate to gather correct rate measurements,^{27,28,32,46} it surely does not identify the liquid molecules in a true physical sense. Other definitions have been proposed and employed,^{47,30} but they usually require more computation time. In any case, relying on a cluster definition inevitably adds another uncertainty to the problem and may lead to a treatment of the cluster which is even less physically correct than before.

Fortunately, the results obtained in the case of argon relieve us from the need of facing these problems, as the deviations we encounter are quite small for nucleation. This finding is in agreement with the results of Tanaka *et al.*, who

also found only negligible difference between results from velocity scaling and a carrier gas.³⁰ Still, our results also suggest that a carrier gas should be used or at least considered under some circumstances. This surely would be the case for a system with stronger interactions or when we are interested in growth rather than nucleation, where Fig. 4 already indicates that we may encounter more serious artifacts due to the thermostat.

VI. CONCLUSIONS

We performed extensive MD simulations of nucleation of LJ argon at two different supersaturations to accurately determine the influence of different thermostats and the importance of nonisothermal effects on nucleation rates. It turns out that carrier gas is more effective than VS or NH thermostats in achieving a good thermalization. Nevertheless, we have obtained deviations in the results of the different thermostats of less than a factor of two, which can be considered as negligible for nucleation, where differences of several orders of magnitude are frequently encountered between different experiments of the same substance and also between experiment and theory.

The excellent cluster statistics acquired in this work allowed us to analyze the cluster temperatures and their distribution for different cluster sizes in more detail. We find that subcritically sized clusters are colder and that postcritically sized clusters are warmer than the bath temperature. In turn, owing to the non-Gaussian distribution of the cluster temperatures, the average cluster temperature is found to be always warmer than the bath temperature. Thus, by carefully distinguishing the average cluster temperature from the most likely ensemble temperature of clusters of a given size, previous seemingly contradictory works on the role of nonisothermal effects and cluster temperature fluctuations^{17,20,18} are found to be correct in their own right once the proper temperature is used. The cluster temperatures can be several degrees different from the bath temperature and these differences are more pronounced for highly supersaturated systems, where nucleation and growth occur so fast that the clusters do not have enough time to get rid of their latent heat. Precisely these large deviations plus the strong temperature fluctuations that are unavoidable for a small system (here the cluster) and the extreme sensitivity of nucleation rates to temperature were the main reason to suspect that nucleation rates under nonisothermal conditions could be violently different from the isothermal ones. Yet, it turns out that the temperature of the clusters is shifted with respect to the bath temperatures in a way that compensates these temperature fluctuations so that, overall, the rate is mostly close to the isothermal one.

All our results seem to confirm the theoretical predictions of the classical work of Feder *et al.*, which was proposed more than 40 years ago. In addition, our results indicate that the choice of the direct thermostat does not have a significant effect on the nucleation rate. Therefore, we may quite safely use velocity scaling as the “least-cost” thermostat in terms of calculation time for the sake of getting better statistics, i.e., observing more nucleation events, and achiev-

ing higher accuracies. However, we should bear in mind that this finding cannot be generalized without caution. First, care should be taken when simulating a system with stronger interaction potentials (i.e., larger latent heat release), e.g., the clustering of metal ions.^{45,48,49} Second, velocity scaling should not be used when we are interested in the growth instead of nucleation because the errors inherited from the direct thermostating become more and more pronounced. In any case, our work settles the basis to estimate the influence of the different thermostats and the importance of the nonisothermal effects on nucleation simulations.

ACKNOWLEDGMENTS

The authors would like to thank Dr. Judith Wölk for fruitful and helpful discussions. One of the authors (J.W.) would like to thank Dr. Stephan Wonzak for support with the simulation software. Computer resources were provided by the Department de Física Fonamental of the University of Barcelona and the Regional Computing Center (RRZK) at the University of Cologne. This work was supported through the “Acciones Integradas Hispano-Alemanas” program of the German Academic Exchange Service (DAAD) and the Spanish DGCyT.

- ¹F. F. Abraham, *Homogeneous Nucleation Theory; The Pretransition Theory of Vapor Condensation* (Academic, New York, 1974).
- ²D. Kashchiev, *Nucleation: Basic Theory with Applications* (Butterworth-Heinemann, Oxford, 2000).
- ³A. Laaksonen, V. Talanquer, and D. W. Oxtoby, *Annu. Rev. Phys. Chem.* **46**, 489 (1995).
- ⁴A. Fladerer and R. Strey, *J. Chem. Phys.* **124**, 164710 (2006).
- ⁵K. Iland, J. Wölk, D. Kashchiev, and R. Strey, *J. Chem. Phys.* (to be published).
- ⁶K. Iland, Ph.D. thesis, Universität zu Köln, 2004.
- ⁷R. Becker and W. Döring, *Ann. Phys.* **24**, 719 (1935).
- ⁸D. W. Oxtoby, *J. Phys.: Condens. Matter* **4**, 7627 (1992).
- ⁹M. P. Allen and D. J. Tildesley, *Computer Simulation of Liquids* (Oxford University Press, Oxford, 1989).
- ¹⁰D. Frenkel and B. Smit, *Understanding Molecular Simulation*, 2nd ed. (Academic, San Diego, 2002).
- ¹¹J. Wedekind, D. Reguera, and R. Strey, *J. Chem. Phys.* **125**, 214505 (2006).
- ¹²R. McFee, *Am. J. Phys.* **41**, 230 (1973).
- ¹³C. Kittel, *Am. J. Phys.* **41**, 1211 (1973).
- ¹⁴R. McFee, *Am. J. Phys.* **41**, 1212 (1973).
- ¹⁵C. Kittel, *Phys. Today* **41** (5), 93 (1988).
- ¹⁶B. B. Mandelbrot, *Phys. Today* **42** (1), 71 (1989).
- ¹⁷I. J. Ford and C. F. Clement, *J. Phys. A* **22**, 4007 (1989).
- ¹⁸R. McGraw and R. A. Laviolette, *J. Chem. Phys.* **102**, 8983 (1995).
- ¹⁹J. C. Barrett, C. F. Clement, and I. J. Ford, *J. Phys. A* **26**, 529 (1993).
- ²⁰B. E. Wyslouzil and J. H. Seinfeld, *J. Chem. Phys.* **97**, 2661 (1992).
- ²¹F. M. Kuni, A. P. Grinin, and A. K. Shchekin, *Physica A* **252**, 67 (1998).
- ²²I. Napari and H. Vehkamäki, *J. Chem. Phys.* **124**, 024303 (2006).
- ²³F. T. Fergusson, R. H. Heist, and J. A. I. Nuth, *J. Chem. Phys.* **115**, 10829 (2001).
- ²⁴A.-P. Hyvarinen, D. Brus, V. Zdimal, J. Smolik, M. Kulmala, Y. Viisanen, and H. Lihavainen, *J. Chem. Phys.* **124**, 224304 (2006).
- ²⁵D. Brus, V. Zdimal, and F. Stratmann, *J. Chem. Phys.* **124**, 164306 (2006).
- ²⁶D. W. Oxtoby and A. Laaksonen, *J. Chem. Phys.* **102**, 6846 (1995).
- ²⁷K. Yasuoka and M. Matsumoto, *J. Chem. Phys.* **109**, 8451 (1998).
- ²⁸K. Laasonen, S. Wonzak, R. Strey, and A. Laaksonen, *J. Chem. Phys.* **113**, 9741 (2000).
- ²⁹S. Toxvaerd, *J. Chem. Phys.* **119**, 10764 (2003).
- ³⁰K. K. Tanaka, K. Kawamura, H. Tanaka, and K. Nakazawa, *J. Chem. Phys.* **122**, 184514 (2005).
- ³¹K. Yasuoka and X. C. Zeng, *J. Chem. Phys.* **126**, 124320 (2007).
- ³²J. Wedekind, R. Strey, and D. Reguera, *J. Chem. Phys.* **126**, 134103 (2007).

- (2007).
- ³³J. Feder, K. C. Russell, J. Lothe, and G. M. Pound, *Adv. Phys.* **15**, 111 (1966).
- ³⁴H. C. Andersen, *J. Chem. Phys.* **72**, 2384 (1980).
- ³⁵J. C. Barrett, *J. Chem. Phys.* **126**, 074312 (2007).
- ³⁶S. Nosé, *J. Chem. Phys.* **81**, 511 (1984).
- ³⁷S. Nosé, *Mol. Phys.* **52**, 255 (1984).
- ³⁸W. G. Hoover, *Phys. Rev. A* **31**, 1695 (1985).
- ³⁹W. G. Hoover, *Phys. Rev. A* **34**, 2499 (1986).
- ⁴⁰G. J. Martyna, D. J. Tobias, and M. L. Klein, *J. Chem. Phys.* **101**, 4177 (1994).
- ⁴¹G. J. Martyna, M. L. Klein, and M. Tuckerman, *J. Chem. Phys.* **97**, 2635 (1992).
- ⁴²S. Wonzak, Ph.D. thesis, Universität zu Köln, 2001.
- ⁴³R. Strey, P. E. Wagner, and Y. Viisanen, *J. Phys. Chem.* **98**, 7748 (1994).
- ⁴⁴W. G. Hoover, B. L. Holian, and H. A. Posch, *Phys. Rev. E* **48**, 3196 (1993).
- ⁴⁵P. Erhart and K. Albe, *Appl. Surf. Sci.* **226**, 12 (2004).
- ⁴⁶S. Toxvaerd, *J. Chem. Phys.* **115**, 8913 (2001).
- ⁴⁷P. R. ten Wolde and D. Frenkel, *J. Chem. Phys.* **109**, 9901 (1998).
- ⁴⁸N. Lümmen and T. Kraska, *Nanotechnology* **16**, 2870 (2005).
- ⁴⁹N. Lümmen and T. Kraska, *Comput. Mater. Sci.* **35**, 210 (2006).
- ⁵⁰R. B. Stewart and R. T. Jacobsen, *J. Phys. Chem. Ref. Data* **18**, 639 (1989).